DOI: 10.55415/deep-2022-0024.v1

Design and synthesis of novel hydroxamic acid derivatives based on quisinostat as promising antimalarial agents with improved safety

Manjiong Wang[1,#], Tongke Tang[2,6,#], Zhenghui Huang[2], Ruoxi Li[1], Dazheng Ling[1], Jin Zhu[1], Lubin Jiang[2,6,*], Jian Li[1,3,4,5*], Xiaokang Li[1,*]

[1]State Key Laboratory of Bioreactor Engineering, Shanghai Frontiers Science Center of Optogenetic Techniques for Cell Metabolism, Frontiers Science Center for Materiobiology and Dynamic Chemistry, Shanghai Key Laboratory of New Drug Design, School of Pharmacy, East China University of Science and Technology, Shanghai 200237, China

[2]Key Laboratory of Molecular Virology and Immunology, Institut Pasteur of Shanghai, University of Chinese Academy of Sciences, Chinese Academy of Sciences, Shanghai 200031, China

[3]Yunnan Key Laboratory of Screening and Research on Anti-pathogenic Plant Resources from West Yunnan, College of Pharmacy, Dali University, Dali 671000, China

[4]Clinical Medicine Scientific and Technical Innovation Center, Shanghai Tenth People's Hospital, Tongji University School of Medicine, Shanghai 200092, China

[5]Key Laboratory of Tropical Biological Resources of Ministry of Education, College of Pharmacy, Hainan University, Haikou 570228, Hainan, China

[6]School of Life Science and Technology, ShanghaiTech University, Shanghai 201210, P.R. China

[#]These authors contributed equally to this work: Manjiong Wang, Tongke Tang.

*e-mail: xkli@ecust.edu.cn; jianli@ecust.edu.cn; lbjiang@ips.ac.cn

DOI: 10.55415/deep-2022-0024.v1

Abstract

In our previous work, the clinical phase II HDAC inhibitor quisinostat was identified as a promising antimalarial agent through drug repurposing strategy, but its safety was of concern. Herein, further medicinal chemistry method was used to find new chemical entities with greater effectiveness and security than quisinostat. Totally, 38 novel hydroxamic acid derivatives were designed and synthesized and their *in vitro* antimalarial activities were systematically investigated. These compounds showed inhibitory effect on wild and drug-resistant *Plasmodium falciparum* strains in erythrocyte stage at nanomole concentrations. Among them, compound **30** displayed completely elimination of parasites in *Plasmodium yoelii* infected mice through oral administration, and also exhibited better safety and metabolic properties compared with our previous work. Moreover, compound **30** was proved that can upregulate the acetylation level of plasmodium histone by western blot, suggesting it exerted antimalarial effect by the inhibition of *Pf*HDAC enzymes.

Keywords: Antimalarial; Drug repurposing; Hydroxamic acid; Erythrocyte stage; Drug resistance

1. Introduction

Malaria is one of the oldest and deadliest infectious diseases and the whole world has never stopped fighting it. According to the World Malaria Report 2021, there were an estimated 241 million cases of malaria and 627,000 deaths from malaria in 2020, an increase of 14 million malaria cases and 69000 deaths compared to 2019 [1]. The rise in malaria cases and deaths has been linked to the disruption of malaria services due to the COVID-19 outbreak in 2019 [2, 3], but global progress against malaria had already stalled before the outbreak. Although

DOI: 10.55415/deep-2022-0024.v1

the world health organization (WHO) recommended widespread use of RTS,S/AS01 vaccine to prevent malaria in young children in African, the vaccine did not provide 100% protection [4]. Under such circumstances, the importance of chemotherapy drugs was highlighted. However, the emergence and spread of drug-resistant malaria has been the biggest public health emergency in malaria control. Especially, the alarming artemisinin-resistant strains have emerged frequently in Southeast Asia and Africa in recent years [5-9], posing a challenge to the first-line therapies, artemisinin-based combination therapies (ACTs) [10]. Therefore, the development of new antimalarial drugs effective against resistant plasmodium is a major scientific and public health problem that needs to be addressed urgently.

In order to solve the problem of drug resistance, medicinal chemists committed to developing new chemical agents with different targets and mechanisms of action in comparison with existing antimalarial drugs [11-15]. A growing number of studies have revealed that histone deacetylase (HDAC) inhibitors have potent killing effect against plasmodium *in vitro* and *in vivo* [16-21]. HDACs play important roles in eukaryotic cellular chromatin structure, transcription and gene expression [22]. Until now, five *Plasmodium falciparum* HDACs (*Pf*HDACs) have been identified, which were related the survival of plasmodium by influencing gene expression, virulence, antigenic variation, and cytoadhesion [23-25].

In our previous studies, a clinical phase II anticancer HDAC inhibitor quisinostat was identified as a promising antimalarial agent but with high toxicity. The structural modification of quisinostat was demonstrated to reduce toxicity while retaining potent antimalarial activity, and further experiments confirmed that its derivatives are *Pf*HDAC inhibitors [26-28]. In

DOI: 10.55415/deep-2022-0024.v1

order to explore new structural framework and further improve the safety to broaden the therapeutic window, new attempts were made in this paper. Referring to the successful experience of previous works, the hydroxamic acid fragment was retained as the zinc-binding group (ZBG) and the 4-aminomethylpiperidine moiety of linker was replaced with 1-oxa-4,9-diazaspiro[5.5]undecane moiety to increase the rigidity of compounds by conformational restriction. The *N*-methylindole fragment (CAP region) was then systematically modified to fully explore the structure-activity relationships (SARs) and further improve bioactivity (**Figure 1**). Finally, 38 derivatives with new structural framework were obtained in total.

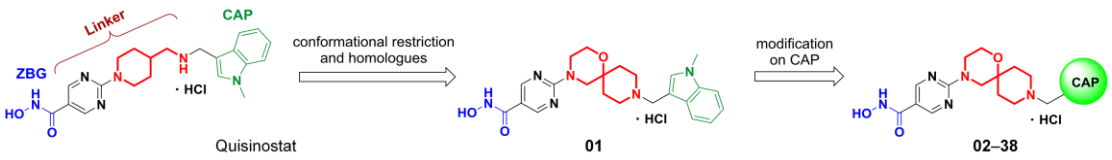

Figure 1. Design of novel hydroxamic acid derivatives.

2. Methods

2.1. Compound synthesis

The synthetic method of compounds **01**–**38** was depicted in **Scheme 1**. Compound **A** was obtained by the nucleophilic aromatic substitution reaction between ethyl 2-chloropyrimidine-5-carboxylate and *tert*-butyl 1-oxa-4,9-diazaspiro[5.5]undecane-9-carboxylate under alkaline conditions, then the *tert*-butoxycarbonyl (Boc) group was removed in the solution of hydrochloric acid/dioxane to obtain compound **B**. Compound **B** underwent reductive amination to yield intermediates **C01**–**C38**. Next, the ethyl ester of **C01**–**C38** was hydrolyzed and then condensed with *O*-(tetrahydro-2H-pyran-2-yl)hydroxylamine ($THPONH_2$) to acquire intermediates **D01**–**D38**.

DOI: 10.55415/deep-2022-0024.v1

Finally, target compounds **01**–**38** were obtained by deprotection in the solution of hydrochloric acid/dioxane. The detailed synthesis and characterization of final compounds **01**–**38** were documented in Supporting Information.

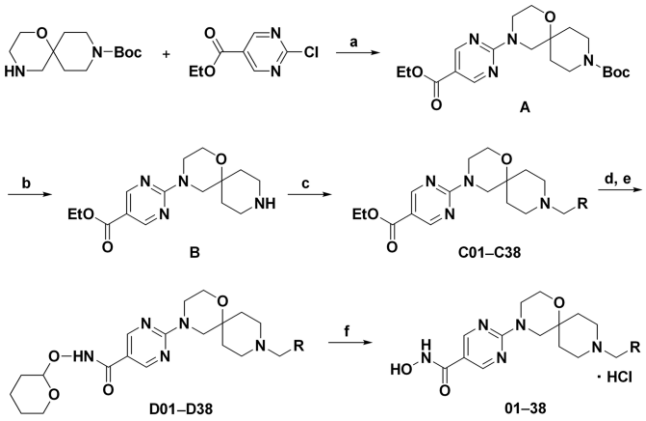

Scheme 1. Synthesis of compounds **01**–**38**. Reagents and conditions: (a) DIPEA, DCM, 0 ℃ to rt, 2–3 h; (b) HCl in 1,4-dioxane , DCM, rt, 5–6 h; (c) RCHO, $NaBH(OAc)_3$, HOAc, DCE, rt, over night; (d) K_2CO_3, MeOH:H_2O = (1:1), 65–70 ℃, 8–12 h; (e) $THPONH_2$, EDCI, HOBt, Et_3N, DMF, rt, 48 h; (f) HCl in 1,4-dioxane, DCM, rt, 30 min.

2.2. Parasite culture

The different strains of parasite used in this work were all cultured by RPMI 1640 medium (Gibco) supplemented with sodium bicarbonate (2.2 g/L), Albumax (5 g/L), HEPES (5.94 g/L), hypoxanthine (50 mg/L), and gentamycin (50 mg/L) in an atmosphere consisting of 5% O_2, 5% CO_2 and 90% N_2 [29].

2.3. *In vitro* 72 h erythrocyte stage parasite-killing assay

Highly synchronized ring-stage parasites (1% parasitemia, and 2% hematocrit) were cuiltured in a 96-well plate with a total volume of 200 μL of compounds. The compounds come from a serial dilution with an initial concentration of 200 nM. After 72 hours incubation, 100 μL of

DOI: 10.55415/deep-2022-0024.v1

dissolution buffer (0.12 mg/mL Saponin, 0.12% Triton X-100, 30 mM Tris-Cl and 7.5 mM EDTA) was added to dissolve the parasites. Then each well was stained with SYBR Green Ⅰ (Invitrogen; supplied as 10,000× dilution) and incubated in the dark for 2 hours [30]. Under 485 nm excitation and 535 nm emission conditions, the fluorescence signal representing the parasite DNA was monitored on the microplate reader (Bioteck, Synergy H1). IC_{50} was calculated by GraphPad 7. The results were shown as the mean ± SD from two independent experiments.

2.4. *In vitro* cytotoxicity assay

HepG2 and 293T cells were cultured in DMEM medium (HyClone) supplemented with 10% FBS (Gibco) and 1% P/S (YEASEN) at 37 ℃ in 5% CO_2. Cells (70,000 cells/mL) were seeded in the 96-well plate in total 100 μL and cultured for 24 h. Tested compounds were added into the plate (concentrations were two-fold dilutions ranging from 20 μM to 0.049 μM) and cells was continuing cultured for 72 h. Then 10% cell counting kit 8 (YEASEN) was added to each well for the analysis of cell viability assay. The absorbance was monitored after 2 h at 450 nm by microplate reader (Bioteck, Synergy H1), IC_{50} was calculated by GraphPad 7. The results were shown as the mean ± SD from two independent experiments.

2.5. Mouse liver microsomes metabolism assay

This experiment was performed by Shanghai ChemPartner Co., Ltd. Liver microsomes (0.5 mg/mL) were purchased from Corning Corporation. Ketanserin was used as a positive control. First, the tested compounds were dissolved in DMSO (10 mM) and then diluted to 0.5 mM with acetonitrile. Dilute the compound to a working concentration of 1.5 μM using liver microsomal buffer, where 30 μL was mixed with 15 μL 6 mM NADPH at 37 ℃. At 0, 5, 15,

DOI: 10.55415/deep-2022-0024.v1

30, 45 minutes after incubation, add 135 μL of acetonitrile to stop the reaction. The mixture was shaken on a shaker (IKA, MTS 2/4) at 600 rpm/min for 10 min, and then centrifuged at 5594×g for 15 min (Thermo Multifuge×3R). The supernatant was diluted 1:1 into distilled water and analyzed by LC-MS/MS.

2.6. *In vivo* erythrocytic antimalarial assay

All animal experimental procedures followed the National Institutes of Health Guide for the Care and Use of Laboratory Animals under the supervision of Animal Welfare and Committee of Institute Pasteur of shanghai, Chinese Academy of Sciences (IACUC Issue No. A2018009). Each group contained five female Balb/c mice (6–8 weeks). At day 0, each mouse was inoculated with 10^5 *P. yoelii* parasites via i.p. [31]. After 24 h, the solution of compounds (DMSO: 20wt% aqueous 2-hydroxypropyl-*β*-cyclodextrin = 5:95 v/v) or solvent was delivered at the indicated dose via i.p. once daily for five successive days. PPQ was used as a positive control. Parasitemia was counted from at least 5,000 RBCs by smearing at day 6, day 30 and day 60. The graph was generated by GraphPad 7.

2.7. Western blot assay

Firstly, the RBC in parasites samples were removed by 0.15% saponin, and then the parasites were sonicated in the 1% NP40-lysis buffer. After centrifugation at 12,000 × g for 15 min, the supernatant was resuspended in a regular SDS-loading buffer. Separate the parasite proteins by 10% SDS-PAGE and transfer to PVDF membrane (Millipore). Use histone H3 acetylation antibody (Millipore; 06-599) or anti-histone H3 antibody (ABclonal; A2348) for Immunodetection, and then use secondary antibody to bind with HRP (Jackson Immuno Research Laboratories). Signal detection was carried out with a chemiluminescent HRP

DOI: 10.55415/deep-2022-0024.v1

substrate Immobilon-Western kit (milipore).

2.8. Human HDAC inhibition assay

This experiment was performed by Shanghai ChemPartner Co., Ltd. Human HDACs 1–3, 6, 8 and SIRT 2 were purchased from BPS. SAHA and suramin were used as positive controls. The tested compound was dissolved in DMSO (20 mM). First, the compound with an initial concentration of 10 μM and triple dilution were incubated with 15 μL enzyme /Tris buffer at room temperature for 15 min. Add 10 μL trypsin and Ac-peptide substrate/Tris buffer to start the reaction, and then incubate 1–3, 6 HDACs at room temperature. 10 μL AC-Peptide substrate /Tris buffer was added to start the reaction and incubated at room temperature for 4 h. Then HDAC 8 and SIRT 2 were incubated with trypsin solution for 2 h. Enzyme activities were measured on Synergy MX excited at 355 nm and emitted at 460 nm. IC_{50} was calculated by GraphPad 7.

2.9. Pharmacokinetic assay

This experiment was performed by Shanghai ChemPartner Co., Ltd. Female Balb/c mice (6–8 weeks) were bred to acclimate for 1 week. The compounds were dissolved in 5% DMSO and diluted to 0.5 mg/ml with 20% aqueous 2-Hydroxypropyl-*β*-cyclodextrin solution as a stock concentration. Each mouse was intraperitoneally injected with a compound solution at a dose of 5 mg/kg. Centrifuge blood samples collected from tubes containing anticoagulant (K2EDTA) at 0.25, 0.5, 1, 2, 4, 8, and 24 h after injection to obtain plasma at 2,000 × g at 4 ℃ for 5 min. The LC-MS/MS of samples were performed on an ACQUITY UPLC HSS T3 1.8 μm column. The mobile phase was a mixture of phase A (0.1% formic acid in water) and phase B (0.1% formic acid in acetonitrile), running in gradient mode at a flow rate of 0.6

DOI: 10.55415/deep-2022-0024.v1

mL/min at 60 ℃. Mass spectra were aquired on an API6500 triple quadrupole equipped with an ESI source. Propranolol were used as the internal standard. Plasma concentration of compound were analyzed, and the pharmacokinetic parameters were calculated via WinNonlin.

3. Results

3.1. *In vitro* inhibition activity, cytotoxicity and SAR of compounds **01**−**38**

In vitro inhibition activity of compounds **01**–**38** were systematically investigated against wild-type *P. falciparum* 3D7 and multidrug-resistant *P. falciparum* Dd2, dihydroartemisinin (DHA) was chose as positive control. In parallel, their cytotoxicity against HepG2 and 293T cells was tested. The results were summarized in **Table 1**. Although the *in vitro* antimalarial activity of most of the compounds was not as good as that of quisinostat, their cytotoxicity was obviously reduced, especially for some compounds with good selectivity indexes greater than 1000. These results suggested that the narrow therapeutic window of quisinostat could be solved by structural modification. Herein, we concluded the following SARs of compounds **01**–**38**: (I) replacing 4-aminomethylpiperidine with 1-oxa-4,9-diazaspiro[5.5]undecane moiety slightly reduced antimalaria activity but observably reduced cytotoxicity (quisinostat *vs* **01**); (II) aliphatic and monocyclic aromatic and biphenyl CAP groups were not conducive to the improvement of antimalarial activity (**02**–**11**, and **15** *vs* **01**); (III) naphthyl, anthryl and other double-aromatic rings are tolerated in the CAP region, except 2-benzothiophenyl. (**12**–**14** and **16**–**26** *vs* **01**); (IV) treatment of azaindolyl group as CAP region or removal of *N*-methyl of 3-indolyl could reduce cytotoxicity and improve selective index (**27**–**33** *vs* **01**); (V) introducing substituent on 3-indolyl group could enhance the potency against Dd2 and the

DOI: 10.55415/deep-2022-0024.v1

selective index for HepG2 cells (**34**–**38** *vs* **01**). In short, some valuable structure-activity and structure-toxicity relationships were obtained through systematic analysis of these 38 hydroxamic acid derivatives; among them, compounds **26**, **33**, **34** and **38** were the four most potent compounds against 3D7 and Dd2 and exhibited improved cellular safety, and compound **30** showed moderate antimalarial activity but the best safety property with selective index > 2316 in two cell lines.

Table 1. *In vitro* asexual erythrocyte stage antimalarial activity and cytotoxicity of compounds **01**–**38**

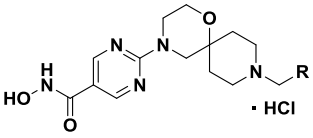

Compd.	R	IC_{50} (nM)[a] against *P. falciparum*		Cytotoxicity IC_{50} (μM)[a]		Selectivity index[b] (3D7)	
		3D7	Dd2	HepG2	293T	HepG2	293T
Quisinostat	-	5.21 ± 1.56	7.09 ± 0.01	0.04 ± 0.01	0.05 ± 0.01	8	9
01		10.51 ± 2.22	14.06 ± 0.11	3.66 ± 0.38	2.13 ± 0.20	349	203
02		107.73 ± 37.72	82.05 ± 4.50	13.85 ± 1.85	8.51 ± 0.46	129	79
03		144.60 ± 21.35	93.30 ± 4.60	> 20	> 20	> 138	> 138
04		62.63 ± 5.25	42.10 ± 5.80	14.33 ± 0.84	14.85 ± 0.61	229	237
05		17.24 ± 3.46	26.47 ± 0.06	4.32 ± 0.06	6.40 ± 2.33	250	371
06		36.13 ± 4.03	72.65 ± 0.28	12.24 ± 0.88	8.62 ± 3.10	339	239
07		56.86 ± 2.81	51.81 ± 1.83	6.25 ± 0.76	7.93 ± 1.30	110	140
08		45.35 ± 3.78	34.66 ± 4.11	9.22 ± 0.23	9.24 ± 1.15	203	204
09		73.99 ± 4.07	202.55 ± 19.87	16.32 ± 2.06	> 20	220	> 270

DOI: 10.55415/deep-2022-0024.v1

10		21.90 ± 2.79	29.89 ± 0.08	19.22 ± 1.57	16.17 ± 0.03	878	738
11		102.90 ± 2.40	54.33 ± 10.22	> 20	> 20	> 194	> 194
12		8.24 ± 0.67	7.95 ± 0.29	3.58 ± 0.38	3.65 ± 0.46	435	443
13		14.59 ± 2.04	8.83 ± 0.78	5.11 ± 0.11	4.59 ± 0.35	350	315
14	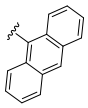	10.94 ± 2.73	9.19 ± 0.46	4.80 ± 0.04	5.83 ± 0.11	439	533
15	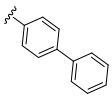	249.30 ± 0.99	88.95 ± 20.58	6.93 ± 0.23	7.83 ± 0.69	28	31
16		10.33 ± 0.37	10.03 ± 0.20	3.13 ± 0.11	5.51 ± 1.77	303	533
17		7.55 ± 1.57	6.93 ± 0.22	3.85 ± 0.13	5.20 ± 0.22	510	688
18		7.28 ± 0.84	6.66 ± 0.58	4.79 ± 0.41	4.21 ± 1.11	657	578
19		7.40 ± 1.13	5.50 ± 0.11	2.12 ± 0.27	2.62 ± 0.50	287	354
20		14.63 ± 0.76	6.73 ± 0.32	2.96 ± 0.40	3.70 ± 0.89	202	253
21		13.28 ± 0.20	12.97 ± 2.04	4.03 ± 0.24	4.21 ± 0.54	303	317
22		14.55 ± 2.21	9.52 ± 0.52	6.22 ± 1.73	6.06 ± 0.93	427	416
23		18.37 ± 0.99	16.55 ± 1.85	8.50 ± 0.04	6.94 ± 1.61	463	378
24		12.14 ± 1.89	12.55 ± 0.48	8.06 ± 0.14	7.46 ± 1.44	664	615
25		46.44 ± 1.67	43.85 ± 0.45	4.09 ± 0.55	7.75 ± 0.20	88	167
26		6.25 ± 0.64	3.86 ± 0.84	2.12 ± 0.12	2.07 ± 0.21	340	331
27		19.39 ± 3.61	13.41 ± 2.14	7.34 ± 2.02	> 20	378	> 1031
28		9.67 ± 0.80	10.75 ± 0.29	3.54 ± 0.57	3.54 ± 0.43	366	366
29		7.50 ± 0.24	10.18 ± 0.39	7.93 ± 0.35	8.32 ± 0.73	819	859

DOI: 10.55415/deep-2022-0024.v1

30		8.64 ± 0.44	26.47 ± 0.06	> 20	> 20	> 2316	> 2316
31		16.58 ± 0.29	19.42 ± 2.92	> 20	12.53 ± 0.792	> 1206	756
32		14.81 ± 1.54	12.25 ± 0.55	8.03 ± 1.00	> 20	542	> 1350
33		5.72 ± 1.02	4.11 ± 0.02	> 20	9.12 ± 0.78	> 3494	1593
34	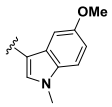	5.36 ± 0.41	3.96 ± 0.29	3.48 ± 0.40	1.26 ± 0.08	648	236
35	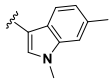	10.49 ± 0.43	6.27 ± 0.39	6.01 ± 1.00	3.48 ± 0.51	573	332
36	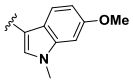	9.79 ± 1.28	4.97 ± 0.57	11.80 ± 1.09	4.07 ± 0.92	1205	416
37	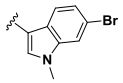	8.80 ± 0.14	6.27 ± 0.59	3.93 ± 0.01	2.65 ± 0.41	446	301
38	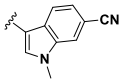	6.49 ± 0.44	3.19 ± 0.09	6.90 ± 0.02	1.75 ± 0.16	1063	269
DHA	-	2.68 ± 0.20	2.67 ± 0.02	nt	nt	nt	nt

[a]IC_{50} values ± standard error of the mean; N = 2; 3D7: sensitive strain; Dd2: multidrug resistance (MDR) strain; DHA: Dihydroartemisinin. [b]Selectivity index (SI) = IC_{50} (cytotoxicity)/IC_{50} (3D7). nt not tested.

3.2. *In vitro* metabolic stability of compounds **26**, **30**, **33**, **34** and **38**

Compounds **26**, **30**, **33**, **34** and **38** were selected to investigate the stability against mouse liver microsomes *in vitro*. As shown in **Table 2**, all texted compounds were more stable than quisinostat. Among them, the half-life ($t_{1/2}$) of **30** was the longest, which was > 150-fold longer than that of quisinostat and > 10-fold longer than compound **33**. These results suggested that the structure of CAP region has a great influence on the metabolic stability.

Table 2. *In vitro* metabolic stability of compounds quisinostat, **26**, **30**, **33**, **34** and **38**

Compd.	metabolic stability in liver microsomes (mouse)

DOI: 10.55415/deep-2022-0024.v1

	$t_{1/2}$ (min)	Cl_{int} (mL/min/kg)
Quisinostat	13.31	410.10
26	23.60	231.26
30	2058.64	2.65
33	200.01	27.29
34	93.88	58.13
38	112.6	48.44

3.3. *In vitro* inhibition activity of compounds **30** and **33** against clinical multidrug-resistant parasites

Compounds **30** and **33**, two of the most stable compounds in mouse liver microsomes, were further evaluated for antimalarial activity against the clinical multi-drug resistant lines (GB4, C2A, CP286, and 6218) via 72 h parasite-killing assay *in vitro*. Their IC_{50}s against the multi-drug resistant lines (**Table 3**) were similar to those of the drug sensitive line 3D7 (**Table 1**), implying that compounds **30** and **33** could avoid the occurrence of cross resistance, which may be related to the difference of antimalarial mechanism between these compounds and existing antimalarial drugs.

Table 3. *In vitro* asexual erythrocyte stage antimalarial activity of compounds **30** and **33** against clinical drug-resistant strains

Compd.	IC_{50} (nM)[a] against *P. falciparum*				
	GB4[b]	C2A[c]	CP286[d]	6218[e]	6320[e]
Quisinostat	1.7 ± 0.1	2.5 ± 0.1	2.0 ± 0.1	1.6 ± 0.0	1.9 ± 0.6
30	13.3 ± 1.6	15.9 ± 2.7	26.6 ± 0.3	14.4 ± 1.3	11.6 ± 1.0
33	10.9 ± 0.3	12.0 ± 1.1	9.3 ± 0.4	8.9 ± 1.3	7.8 ± 0.1
DHA	3.2 ± 1.2	3.7 ± 2.3	5.6 ± 2.3	5.9 ± 2.1	5.2 ± 3.7

[a]IC_{50} values ± standard error of the mean; N =2; [b]drug resistance to chloroquine; [c]drug resistance to

DOI: 10.55415/deep-2022-0024.v1

quinine; [d]drug resistance to sulfadoxine-pyrimethamine and mefloquine; [e]drug resistance to artemisinin.

3.4. Compounds **30** and **33** up-regulated histone acetylation in *P. falciparum* parasites

The mechanism of action of compounds **30** and **33** was explored by western blot to detect the acetylation level of plasmodium histones (**Figure 2**). Plasmodium was pre-incubated with quisinositat, compounds **30** and **33** at 20 fold of IC_{50} concentration for 4 h and the protein of plasmodium was extracted to assess acetylation of histone 3 (H3). Compared with the DMSO blank group, the histone acetylation levels of H3 in the drug-treated group were all up-regulated, especially compound **30**-treated group. It was preliminarily proved that the mechanism of action of these compounds was to inhibit the *Pf*HDAC enzyme, which was the same as our previous work.

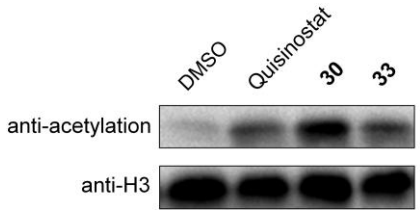

Figure 2. The acetylation of *P. falciparum* histones.

3.5. *In vitro* inhibition activity of compounds **30** and **33** against human HDACs

In addition, the enzyme inhibitory activities of compounds **30** and **33** against human HDACs were also investigated. Among the tested enzymes, HDAC1-3 and HDAC8 are class I HDACs, HDAC6 is belong to class II HDAC, and SIRT2 is a NAD^+-dependent class III HDAC [32]. As can be seen from **Table 4**, the activities of compounds **30** and **33** against class I/II HDACs were remarkably decreased compared with the lead compound quisinostat. This may be one of the reasons for the reduced cytotoxicity of the derivatives in this work.

DOI: 10.55415/deep-2022-0024.v1

Especially, for compound **30**, the IC_{50} values against HDAC1 decreased by nearly 60 times than quisinostat.

Table 4. IC_{50} of compounds **30** and **33** on human HDACs[a]

Compd.	IC_{50} (nM)					
	HDAC 1	HDAC 2	HDAC 3	HDAC 6	HDAC 8	SIRT 2
Quisinostat	< 0.5	1.1	2.1	34.9	9.2	>10000
30	27.4	38.9	103.7	132.5	216.2	>10000
33	10.2	15.1	45.2	66.0	150.8	>10000
Vorinostat	10.5	23.7	27.6	13.5	300.9	nt
Suramin	nt	nt	nt	nt	nt	5441

[a]Vorinostat and suramin were used as positive control drugs. nt not tested.

3.6. *In vivo* asexual erythrocyte stage antimalarial activity of compound **30**

According to the *in vitro* experimental data, compound **30** with low cytotoxicity and the best metabolic stability of liver microsomes was selected as candidate compound to evaluate its efficacy in the *Plasmodium yoelii* infected mice model (**Figure 3**). Herein, BALB/c mice were randomly divided into 5 groups, and the tested drugs were given for 5 running days after the day inoculated with 1×10^5 parasites. Piperaquine phosphate (PPQ) was chose as positive control and administered intraperitoneally, while quisinostat and compound **30** were administered orally. As shown in **Figure 3A**, all mice in the vehicle group died until day 7, indicating successful infection with *P. yoelii*. One mouse in the quisinostat-treated group died on day 6, presumably due to cumulative toxicity caused by continuous administration, while compound **30** showed good safety profile and no mice died. We took blood from the tail of mice on day 6 (the first day after the end of drug administration), day 30 and day 60 and made blood smears to quantify parasitemia, and the results were shown in **Figure 3B**. Although

DOI: 10.55415/deep-2022-0024.v1

compound **30** did not completely kill the parasites on day 6, its parasitemia rates (3.13% in the 120 mg/kg group and 0.12% in the 150 mg/kg group) were obviously lower that of vehicle group (95.23%), indicating that the killing rates were over 95%. Notably, no parasite was observed in mice on day 30 and day 60, proving that all the surviving mice had been cured. Overall, compound **30** was shown to be safe and effective in this model.

A

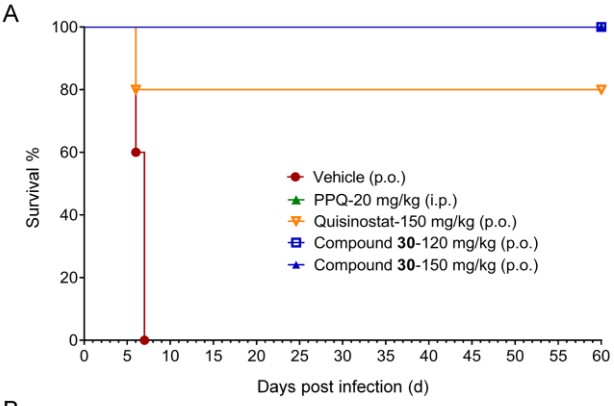

B

Compd.	Administration	Dose (mg/kg)	Parasitemia (%)			Survival (%)
			Day 6[b]	Day 30	Day 60	
Vehicle	p.o.	/	95.23	/	/	0
PPQ[a]	i.p.	20	0	0	0	100
Quisinostat	p.o.	150	0	0	0	80
30		120	3.13	0	0	100
		150	0.12	0	0	100

Figure 3. *In vivo* studies on a murine *P. yoelii* model. (A) Survival ratio. (B) Summary of activities of compounds against *P. yoelii* infection in mice. [a]PPQ, piperaquine phosphate; [b]the day after the end of drug administration.

3.7. *In vivo* asexual erythrocyte stage antimalarial activity of compound **30**

The pharmacokinetic (PK) properties of compound **30** were further investigated in BALB/c mice via intraperitoneal injection (**Table 5**). The maximum concentration (C_{max}) and area under the curve (AUC) of **30** were much higher than those of quisinostat. Higher plasma concentration may result in more potent parasite killing *in vivo*. In addition, compound **30**

DOI: 10.55415/deep-2022-0024.v1

also displayed a slightly longer half-life ($t_{1/2}$) than quisinostat, and it was the preferred derivative with the longest $t_{1/2}$ in the whole series.

Table 5. PK parameters of compounds quisinostat and **30**

Parameter[a]	Quisinostat[b]	**30**
C_{max}(ng/mL)	89	1112
T_{max}(h)	0.08	0.25
AUC_{last}(h*ng/mL)	157	1371
AUC_{inf}(h*ng/mL)	180	1391
$t_{1/2}$(h)	6.13	6.85
CL_Z/F(L/h/kg)	27.72	3.59
V_Z/F(L/kg)	245	35.53

[a]PK parameters in plasma following a single i.p. of 5 mg/kg compound in mice; C_{max}: maximum plasma or hepatic concentration; T_{max}: time to C_{max}; AUC_{last}: area under the concentration−time curve from 0 up to the last sampling time at which a quantifiable concentration is found; AUC_{inf}: area under the concentration−time curve from 0 up to infinity; $t_{1/2}$: apparent elimination half-life; CL_z/F: apparent clearance; V_z/F: apparent volume of distribution [b]Data previously reported [26].

4. Discussion

In this work, we designed and synthesized a series of novel hydroxamic acid derivertives (**01**–**38**) based on antitumor drug quisinostat as antimalarial lead compound. The optimal compound **30** possessed potent inhibitory activity against *P. falciparum* parasites (IC_{50} = 8.64 ± 0.44 nM against 3D7), and low cytotoxicity (IC_{50} > 20 μM against HepG2 and 293T). Further evaluations indicated **30** exhibited strong killing efficacy against several multi-drug resistant clinical *P. falciparum* strains, which may contribute to solve the treatment failure caused by drug resistance. Moreover, the *in vivo* efficacy of compound **30** was demonstrated

DOI: 10.55415/deep-2022-0024.v1

with fully elimination of parasites in the murine *P. yoelii* model and the superior safety profile than the lead compound quisinostat was proved in the same experiment. In addition, **30** exhibited good metabolic stability in liver microsomes and good PK properties in mice. Preliminary mechanism research showed that **30** killed *P. falciparum* parasites by inhibiting *Pf*HDAC enzymes activity. Taken together, all these results warranted **30** was a prospective prototype against malaria therapy and deserved further optimization.

Acknowledgments

We thank Dr. Didier Ménard for providing the artemisinin-resistant field isolates. This work was supported by the National Natural Science Foundation of China (82173689, 22037002, 81872747, 81903457, 31972169), the National Key R&D Program of China (2017YFB0202600), the National Science and Technology Major Project (2018ZX10101004003001), the Key Collaborative Research Program of the Alliance of International Science Organizations (ANSO-CR-KP-2020-06), the Shanghai Frontiers Science Center of Optogenetic Techniques for Cell Metabolism (Shanghai Municipal Education Commission), the Innovative Research Team of High-level Local Universities in Shanghai, the Chinese Special Fund for State Key Laboratory of Bioreactor Engineering (2060204), the Pu'er Municipal Expert Workstation of L. J., the Shanghai Sailing Program (19YF1412600).

Conflict of interest

The authors declare that they have no known competing financial interests or personal relationships that could have appeared to influence the work reported in this paper.

DOI: 10.55415/deep-2022-0024.v1

References

1. *World malaria report 2021*. World Health Organization; 2021.
2. Hakizimana D, Ntizimira C, Mbituyumuremyi A, Hakizimana E, Mahmoud H, Birindabagabo P, et al.: **The impact of Covid-19 on malaria services in three high endemic districts in Rwanda: a mixed-method study.** *Malaria Journal* 2022, 21:48-64.
3. Teboh-Ewungkem MI, Ngwa GA: **COVID-19 in malaria-endemic regions: potential consequences for malaria intervention coverage, morbidity, and mortality.** *The Lancet Infectious Diseases* 2021, 21:5-6.
4. Duffy PE: **Making a good malaria vaccine better.** *Trends in Parasitology* 2022, 38:9-10.
5. Achan J, Mwesigwa J, Edwin CP, D'Alessandro U: **Malaria medicines to address drug resistance and support malaria elimination efforts.** *Expert Review of Clinical Pharmacology* 2018, 11:61-70.
6. Balikagala B, Fukuda N, Ikeda M, Katuro OT, Tachibana SI, Yamauchi M, et al.: **Evidence of Artemisinin-Resistant Malaria in Africa.** *New England Journal of Medicine* 2021, 385:1163-1171.
7. Uwimana A, Legrand E, Stokes BH, Ndikumana JM, Warsame M, Umulisa N, et al.: **Emergence and clonal expansion of *in vitro* artemisinin-resistant *Plasmodium falciparum* kelch13 R561H mutant parasites in Rwanda.** *Nature Medicine* 2020, 26:1602-1608.
8. Dondorp AM, Yeung S, White L, Nguon C, Day NP, Socheat D, et al.: **Artemisinin**

DOI: 10.55415/deep-2022-0024.v1

resistance: current status and scenarios for containment. *Nature Reviews Microbiology* 2010, 8:272-280.

9. Ashley EA, Phyo AP: **Drugs in development for malaria.** *Drugs* 2018, 78:861-879.
10. van der Pluijm RW, Amaratunga C, Dhorda M, Dondorp AM: **Triple artemisinin-based combination therapies for malaria - a new paradigm?** *Trends in Parasitology* 2021, 37:15-24.
11. Phillips MA, Lotharius J, Marsh K, White J, Dayan A, White KL, et al.: **A long-duration dihydroorotate dehydrogenase inhibitor (DSM265) for prevention and treatment of malaria.** *Science Translational Medicine* 2015, 7:296ra111.
12. Paquet T, Le Manach C, Cabrera DG, Younis Y, Henrich PP, Abraham TS, et al.: **Antimalarial efficacy of MMV390048, an inhibitor of *Plasmodium* phosphatidylinositol 4-kinase.** *Science Translational Medicine* 2017, 9:eaad9735.
13. Jimenez-Diaz MB, Ebert D, Salinas Y, Pradhan A, Lehane AM, Myrand-Lapierre ME, et al.: **(+)-SJ733, a clinical candidate for malaria that acts through ATP4 to induce rapid host-mediated clearance of *Plasmodium*.** *Proceedings of the National Academy of Sciences of the United States of America* 2014, 111:E5455-5462.
14. Yang YQ, Yu Y, Li XL, Li J, Wu Y, Yu J, et al.: **Target elucidation by cocrystal structures of nadh-ubiquinone oxidoreductase of *Plasmodium falciparum* (*Pf*NDH2) with small molecule to eliminate drug-resistant malaria.** *Journal of Medicinal Chemistry* 2017, 60:1994-2005.
15. Zhan WH, Visone J, Ouellette T, Harris JC, Wang R, Zhang H, et al.: **Improvement of asparagine ethylenediamines as anti-malarial *Plasmodium*-selective proteasome**

DOI: 10.55415/deep-2022-0024.v1

inhibitors. *Journal of Medicinal Chemistry* 2019, 62:6137-6145.

16. Koehne E, Kreidenweiss A, Zoleko Manego R, McCall M, Mombo-Ngoma G, Mackwitz MKW, et al.: **Histone deacetylase inhibitors with high *in vitro* activities against *Plasmodium falciparum* isolates collected from Gabonese children and adults.** *Scientific Reports* 2019, 9:17336.
17. Chua MJ, Arnold MS, Xu W, Lancelot J, Lamotte S, Spath GF, et al.: **Effect of clinically approved HDAC inhibitors on *Plasmodium, Leishmania* and *Schistosoma* parasite growth.** *International Journal of Parasitology: Drugs and Drug Resistance* 2017, 7:42-50.
18. Hansen FK, Sumanadasa SDM, Stenzel K, Duffy S, Meister S, Marek L, et al.: **Discovery of HDAC inhibitors with potent activity against multiple malaria parasite life cycle stages.** *European Journal of Medicinal Chemistry* 2014, 82:204-213.
19. Beus M, Rajic Z, Maysinger D, Mlinaric Z, Antunovic M, Marijanovic I, et al.: **SAHAquines, novel hybrids based on saha and primaquine motifs, as potential cytostatic and antiplasmodial agents.** *ChemistryOpen* 2018, 7:624-638.
20. Diedrich D, Stenzel K, Hesping E, Antonova-Koch Y, Gebru T, Duffy S, et al.: **One-pot, multi-component synthesis and structure-activity relationships of peptoid-based histone deacetylase (HDAC) inhibitors targeting malaria parasites.** *European Journal of Medicinal Chemistry* 2018, 158:801-813.
21. Mackwitz MKW, Hesping E, Eribez K, Scholer A, Antonova-Koch Y, Held J, et al.: **Investigation of the *in vitro* and *in vivo* efficacy of peptoid-based HDAC inhibitors with dual-stage antiplasmodial activity**. *European Journal of Medicinal Chemistry*

DOI: 10.55415/deep-2022-0024.v1

2021, 211:113065.

22. Huang YH, Dong GQ, Li HQ, Liu N, Zhang WN, Sheng CQ: **Discovery of janus kinase 2 (JAK2) and histone deacetylase (HDAC) dual inhibitors as a novel strategy for the combinational treatment of leukemia and invasive fungal infections**. *Journal of Medicinal Chemistry* 2018, 61:6056-6074.
23. Andrews KT, Haque A, Jones MK: **HDAC inhibitors in parasitic diseases.** *Immunology & Cell Biology* 2012, 90:66-77.
24. Chaal BK, Gupta AP, Wastuwidyaningtyas BD, Luah YH, Bozdech Z: **Histone deacetylases play a major role in the transcriptional regulation of the *Plasmodium falciparum* life cycle.** *PLoS Pathogens* 2010, 6:e1000737.
25. Mancio-Silva L, Lopez-Rubio JJ, Claes A, Scherf A: **Sir2a regulates rDNA transcription and multiplication rate in the human malaria parasite *Plasmodium falciparum*.** *Nature Communications* 2013, 4: 1530-1535.
26. Huang ZH, Li RX, Tang TK, Ling DZ, Wang MJ, Xu DD, et al.: **A novel multistage antiplasmodial inhibitor targeting *Plasmodium falciparum* histone deacetylase 1.** *Cell Discovery* 2020, 6:93-107.
27. Li RX, Ling DZ, Tang TK, Huang ZH, Wang, MJ, Ding, Y, et al.: **Discovery of novel *Plasmodium falciparum* HDAC1 inhibitors with dual-stage antimalarial potency and improved safety based on the clinical anticancer drug candidate Quisinostat.** *Journal of Medicinal Chemistry* 2021, 64:2254-2271.
28. Li RX, Ling DZ, Tang TK, Huang ZH, Wang, MJ, Mao F, et al.: **Repurposing of antitumor drug candidate Quisinostat lead to novel spirocyclic antimalarial agents.**

DOI: 10.55415/deep-2022-0024.v1

Chinese Chemical Letters 2021, 32:1660-1664.

29. Jiang LB, Mu JB, Zhang QF, Ni T, Srinivasan P, Rayavara K, et al.: ***Pf*SETvs methylation of histone H3K36 represses virulence genes in *Plasmodium falciparum*.** *Nature* 2013, 499:223–227.
30. Smilkstein M, Sriwilaijaroen N, Kelly JX, Wilairat P, Riscoe M: **Simple and inexpensive fluorescence-based technique for high-throughput antimalarial drug screening.** *Antimicrobial Agents and Chemotherapy* 2004, 48:1803–1806.
31. Ishih A, Kawakami C, Todoroki A, Hirai H, Ohori K, Kobayashi F: **Outcome of primary lethal and nonlethal *Plasmodium yoelii* malaria infection in BALB/c and IFN-gamma receptor-deficient mice following chloroquine treatment.** *Parasitology Research* 2013, 112:773-780.
32. Varasi M, Thaler F, Abate A, Bigogno C, Boggio R, Carenzi G, et al.: **Discovery, synthesis, and pharmacological evaluation of spiropiperidine hydroxamic acid based derivatives as structurally novel histone deacetylase (HDAC) inhibitors.** *Journal of Medicinal Chemistry* 2011, 54:3051-3064.